

# Signatures of charmonium modification in spatial correlation functions

F. Karsch,<sup>1,2,\*</sup> E. Laermann,<sup>1,†</sup> Swagato Mukherjee,<sup>2,‡</sup> and P. Petreczky<sup>2,§</sup>

<sup>1</sup>*Fakultät für Physik, Universität Bielefeld, Bielefeld 33615, Germany*

<sup>2</sup>*Brookhaven National Laboratory, Upton NY 11973, USA*

## Abstract

We study spatial correlation functions of charmonium in 2+1 flavor QCD using an improved staggered formulation. Contrary to the temporal correlation functions the spatial correlation functions exhibit a strong temperature dependence above the QCD transition temperature. Above this temperature they are sensitive to temporal boundary conditions. Both features become significant at a temperature close to  $1.5T_c$  and suggest corresponding modifications of charmonium spectral functions.

PACS numbers: 11.15.Ha, 12.38.Aw

---

\*E-mail: karsch@bnl.gov

†E-mail: edwin@physik.uni-bielefeld.de

‡E-mail: swagato@bnl.gov

§E-mail: petreczk@bnl.gov

## I. INTRODUCTION

Quarkonium suppression was proposed long ago by Matsui and Satz as a signal for deconfinement in heavy ion collisions [1]. The basic idea behind this proposal was the fact that at sufficiently high temperatures color screening will prevent formation of heavy quark bound states (for recent reviews on this topic see [2, 3]). Charmonium suppression was indeed observed in heavy ion experiments at SPS [4] and at RHIC [5], and is now being intensively studied also at the LHC [6]. In order to interpret current and future experimental findings it is very important to know (among other things) the in-medium properties of heavy quark anti-quark pairs.

The notion of bound state melting can be rigorously formulated in terms of the spectral functions. Charmonium dissociation corresponds to gradual broadening and eventual disappearance of the bound state peaks in the corresponding meson spectral functions. Spectral functions are related to the Euclidean time meson correlation functions and can be studied using lattice QCD calculations. The standard approach to obtain information about the spectral functions from calculations of temporal correlators relies on the Maximum Entropy Method (MEM) [7, 8]. Based on this approach, analyses in quenched QCD led to the conclusion that 1S charmonium states may survive up to temperatures as high as  $1.6T_c$ , with  $T_c$  being the deconfinement temperature of the SU(3) gauge theory [9–12] (for a similar analysis in 2 flavor QCD see [13]). Other lattice QCD studies based on different techniques, e.g. variational analysis, led to similar conclusions [14, 15]. The conclusion that charmonium states survive in a certain temperature range above the QCD transition temperature is largely based on the observation that the corresponding temporal meson correlation functions show a weak temperature dependence across the transition [11, 12, 16–18]. Moreover, at high temperatures in particular the vector spectral function receives a contribution near zero frequency,  $\omega \simeq 0$ , which corresponds to the transport of heavy quarks. This near-zero-mode of the spectral function gives rise to a contribution to the temporal correlation function that is (almost) constant in Euclidean time and is responsible for most of the temperature dependence of temporal meson correlators [16, 17]. Thus, the temperature dependent effects due to in-medium modifications and dissolution of charmonium states appear to be small in

temporal correlation functions <sup>1</sup>

Contrary to the lattice analysis of temporal meson correlators, potential model studies that use the static quark anti-quark correlators calculated in lattice QCD [20] as an input into the Schrödinger equation, predict melting of charmonium bound states at temperatures slightly above the QCD transition temperature [21–23]. Furthermore, analyses of quarkonia at non-zero temperature within the effective field theory approach revealed that in addition to the modification of its real part, the potential also acquires an imaginary part [24, 25]. The imaginary part plays an important role in quarkonium dissociation. Even when one takes into account the uncertainties in relating the imaginary part of the potential to the correlation functions of a static quark anti-quark pair calculated in lattice QCD, a non-vanishing imaginary part leads to the dissolution of at least the charmonium bound states [26]. A similar conclusion was reached in the analysis of the charmonium spectral functions using the T-matrix approach [27]. Remarkably though, it was shown in the framework of potential models that the melting of quarkonium states does not result in large changes of the temporal correlators and the correlators seemed to be temperature independent to very good approximation [22]. Thus both potential models and direct lattice QCD calculations suggest only a weak temperature dependence of the temporal meson correlators across the transition.

In order to extract detailed features of the spectral functions, *e.g.* broadening of bound state peaks or melting of states, from such weakly temperature dependent temporal correlators one needs high precision data at a large number of Euclidean time separations. The most recent high statistics (quenched) lattice calculation of charmonium spectral functions using MEM reached lattice spacings down to  $a = 0.01$  fm [18]. This study found no evidence for bound state peaks at  $T \simeq 1.46T_c$ , suggesting charmonium melting to take place at a temperature somewhat smaller compared to the earlier MEM based lattice QCD analyses. Nevertheless, it is desirable to have alternative observables that may provide additional information on the in-medium properties of heavy quark bound states.

In this paper we therefore analyze spatial charmonium correlators at non-zero temperature. Following [28] we also study the dependence of the spatial meson correlation functions

---

<sup>1</sup> Using NRQCD at finite temperature some evidence for melting of bottomonium P-states, that have same size as the ground state charmonium, was obtained [19].

on the temporal boundary condition. We have found that the behavior of spatial charmonium correlators and their dependence on the boundary condition is consistent with significant modifications of charmonium states at sufficiently high temperatures. Some preliminary results of this work were presented previously in [29, 30]. We also note that some exploratory studies of spatial charmonium correlators in quenched QCD were reported in [11]. Our findings in 2+1 flavor QCD are qualitatively consistent with these calculations.

## II. SPATIAL CORRELATION FUNCTIONS

Correlation functions of a meson operator  $J = \bar{q}\Gamma q$  along the spatial direction  $z$  are defined as

$$G(z, T) = \int dx dy \int_0^{1/T} d\tau \langle J(x, y, z, \tau) J(0, 0, 0, 0) \rangle. \quad (1)$$

The matrix  $\Gamma$  is a product of Dirac matrices and fixes the quantum number of the meson. The spatial correlation function is related to the meson spectral function at non-zero spatial momentum

$$G(z, T) = \int_0^\infty \frac{2d\omega}{\omega} \int_{-\infty}^\infty dp_z e^{ip_z z} \sigma(\omega, p_z, T) \quad (2)$$

Thus the temperature dependence of the spatial correlation function also provides information about the temperature dependence of the spectral function. Medium effects are expected to be the largest at distances that are larger than  $1/T$ . At these distances  $G(z, T)$  decays exponentially and this exponential decay is governed by a screening mass  $M_{scr}$ . It is also pertinent to note here that the above relation suggests, unlike the temporal correlation functions, an  $\omega\delta(\omega)$  type zero-mode contribution to the spectral function does not lead to a non-decaying constant contribution to the spatial correlation functions and only leads to a contact term.

If there is a lowest lying meson state of mass  $M$ , this is signaled by a peak in the spectral function,  $\sigma(\omega, p_z, T) \sim \delta(\omega^2 - p_z^2 - M^2)$ . This bound state peak in the spectral function determines the long distance behavior of the spatial meson correlation function. We thus have  $M_{scr} = M$ . On the other hand, at very high temperatures the charm quark and anti-quark are not bound and the meson screening mass is given by  $2\sqrt{(\pi T)^2 + m_c^2}$ , where  $m_c$  is the charm quark mass and  $\pi T$  is the lowest fermionic Matsubara frequency. The above value of the screening mass is a consequence of the anti-periodicity of the fermion fields along the time direction and forces the charm quark (anti-quark) to pick up at least a  $\pi T$

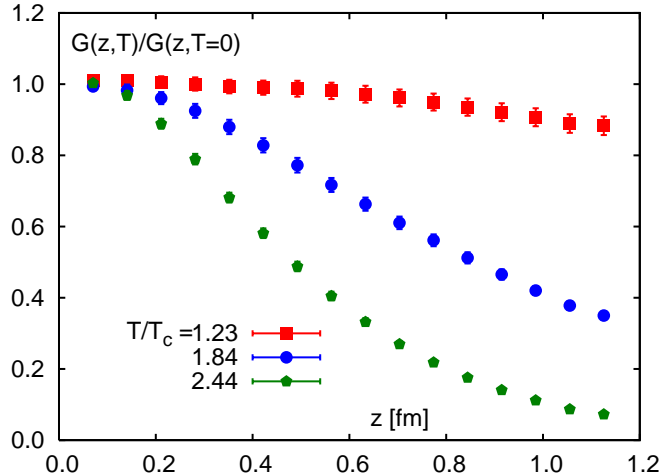


FIG. 1: Ratio of the spatial pseudo-scalar correlators to the corresponding zero temperature correlators calculated for  $a^{-1} = 2.8$  GeV at three different temperatures. Calculations have been performed on lattices with temporal extent  $N_\tau = 6, 8,$  and  $12$ . In units of the transition temperature, these correspond to  $T/T_c = 1.23, 1.84,$  and  $2.44$ .

contribution from the lowest non-vanishing Matsubara frequency at non-zero temperatures. The transition between these two limiting behaviors of the screening masses may serve as an indicator for significant modifications and ultimately dissolution of the meson states.

Furthermore, if the  $c\bar{c}$  pair forms a mesonic bound state the screening mass is not expected to be sensitive to the anti-periodic temporal boundary condition due to the bosonic nature of the basic degrees of freedom. In this case using a periodic temporal boundary condition for the fermions is expected to give the same screening mass as for the case of an anti-periodic temporal boundary condition. Since for the non-interacting theory with a periodic temporal boundary condition  $M_{scr} = 2m_c$ , a comparison with the usual anti-periodic case of  $M_{scr} = 2\sqrt{(\pi T)^2 + m_c^2}$  will also facilitate in the identification of free theory like behavior of the spatial correlation functions. Thus studying the dependence of the screening masses on the temporal boundary conditions may also provide some additional information about the existence of bound states.

### III. NUMERICAL RESULTS

We performed numerical calculations in 2+1 flavor QCD using the improved staggered p4 action [32, 33] on  $32^3 \times N_\tau$  lattices with  $N_\tau = 6, 8, 12$  and 32. Some calculations have also been performed on  $24^3 \times 6$  lattice. We mostly used the gauge field configurations generated for the study of the QCD equation of state [34, 35]. The strange quark mass  $m_s$  was fixed to its physical value, while for the light quark masses we used  $m_s/10$  corresponding in the continuum limit to a pion mass of about 220 MeV. The lattice spacing was fixed using the value  $r_0 = 0.469$  fm [36] for the Sommer scale [37]. A detailed discussion of the choice of the lattice parameters is given in Refs. [34, 35]. Since for lattice spacings used in this study cutoff effects may be still significant we will present our results in terms of the reduced temperature  $T/T_c$ . For the transition temperature for  $N_\tau = 6$  and 8 lattices we will use the values  $T_c = 198$  MeV and  $T_c = 191$  MeV from Ref. [38, 39]. From the  $O(N)$  scaling analysis presented in [39] we estimate  $T_c \simeq 160$  MeV in the continuum limit for light quark masses of  $m_s/10$ . Assuming a  $1/N_\tau^2$  dependence of  $T_c$  for  $N_\tau > 8$  we estimate that  $T_c \simeq 174$  MeV for  $N_\tau = 12$ . We also used the staggered p4 action for the valence charm sector. The valence charm quark masses were fixed to reproduce the physical value of the  $J/\psi$  mass at  $T = 0$  [40, 41].

The staggered fermion formulation describes four valence quark flavors in the continuum limit. Meson operators in this formalism are written as  $J = \bar{q}(\Gamma^D \times \Gamma^F)q$ , where  $\Gamma^D$  and  $\Gamma^F$  are products of the Dirac matrices and describe the spin flavor structure of the meson [42]. Here we consider only local meson operators for which  $\Gamma^D = \Gamma^F = \Gamma$ , since these are the cheapest to calculate. As in most lattice QCD studies only the quark-line connected part of the correlation function is taken into account; however, for heavy quarks the effect due to the disconnected part is expected to be small. The meson operators can be written in terms of staggered quark fields,  $\chi$  and  $\bar{\chi}$  as  $J = \tilde{\phi}(X)\bar{\chi}(X)\chi(X)$ ,  $X = (x, y, z, \tau)$  [43, 44]. Different meson channels/operators are fixed by appropriate choice of the phase factor  $\tilde{\phi}(X)$ . Each choice of  $\tilde{\phi}(X)$  corresponds to a pair of  $\Gamma$  matrices related to positive and negative parity states that show up as oscillatory and non-oscillatory terms in the correlation function [44]. In our analysis we used both point and wall sources.

In this paper we mainly discuss the simplest case corresponding to  $\tilde{\phi}(X) = -(-1)^{\tau+x+y}$ . We will comment on other choices of  $\tilde{\phi}(X)$  later. The correlator corresponding to  $\tilde{\phi}(X) =$

$-(-1)^{\tau+x+y}$  is dominated only by pseudo-scalar meson states (the oscillatory contribution vanishes) and thus is the easiest to analyze. For this reason we refer to the corresponding correlator as the pseudo-scalar correlator. In the zero temperature limit this correlator corresponds to the spin singlet S-wave charmonium state  $\eta_c$ . First we are interested in the change of the correlation functions in the high temperature regime of QCD relative to the zero temperature correlator. In Fig. 1 we show the ratio of the spatial correlators calculated for three different temperatures corresponding to  $N_\tau = 6, 8$  and  $12$  and for fixed lattice spacing  $a^{-1} = 2.8$  GeV. As one can see from the figure the correlator shows significant change already at a temperature of  $T/T_c \simeq 1.2$ . As the temperature increases further the deviations from the zero temperature correlator become more prominent. This is different from the case of the temporal correlators, where very little change is seen even at the highest temperature. This is partly due to the fact that larger separations can be probed in the spatial direction. Indeed, for separations smaller than  $1/(2T)$ , available in the case of temporal correlators, the temperature dependence is very moderate.

We have studied the long distance behavior of the spatial correlators and using simple exponential fits extracted the corresponding screening masses as well as the amplitudes. In the zero temperature limit the latter are proportional to the square of the wave functions at the origin. At infinite temperature, i.e. in the free case limit, the leading behavior of the correlation function has the form  $\sim e^{-m_{scr}z}/z$  [45]. However, a  $1/z$  dependence of the amplitude or, corrolary, a decrease of the effective screening mass  $m_{scr}(z) = \ln G(z)/G(z+1)$  proportional to  $\ln(1+1/z) \simeq 1/z$  has not been observed.

In Fig. 2 we show the screening masses and the amplitudes divided by the corresponding zero temperature values as function of temperature in units of the transition temperature  $T_c$ . As one can see from the figure the cutoff effects for the screening masses and the corresponding amplitude are small. At low temperatures both the masses and the amplitudes agree with their  $T = 0$  values within errors. Above the transition temperature we see small but statistically significant deviations from the zero temperature result. We also compare our numerical results for the screening masses for  $T > 1.2T_c$  with the free theory result  $2\sqrt{(\pi T)^2 + m_c^2}$ . Here we used  $m_c = 1.42$  GeV, as will be justified later.

For  $T > 1.5T_c$  deviations from the zero temperature limit become large and the screening masses are compatible with the behavior characteristic for unbound  $c\bar{c}$  pairs. The behavior of the charmonium screening masses is very similar to the findings of a study in quenched

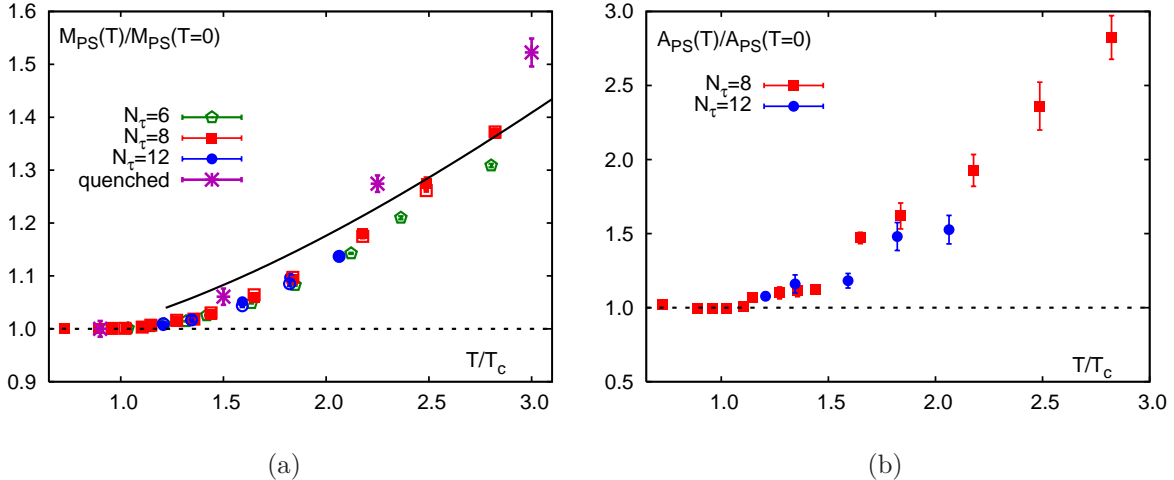


FIG. 2: Pseudo-scalar screening mass (a) and amplitude (b) divided by the corresponding zero temperature values as function of the temperature. Filled symbols show the results obtained with point sources, while open symbols represent the results from the wall sources. The quenched results are taken from Ref. [11] and correspond to the smallest lattice spacing ( $a^{-1} \simeq 9.7$  GeV) used in that study. (This corresponded to lattices with temporal extent  $N_\tau = 12, 16,$  and  $24$ ). The solid black line is the free quark result (see text for details).

QCD [11]. The change in the temperature dependence of the charmonium screening masses around  $T = 1.5T_c$  is similar to the change of the screening masses in the light quark sector around the QCD transition temperature [31]. Therefore the change in the behavior of the charmonium screening masses around  $T = 1.5T_c$  is likely due to the melting of the meson states.

As stated above, the dependence of the screening masses on the temporal boundary conditions can provide additional information about the existence of bound states in the deconfined medium. Therefore, we also calculated the pseudo-scalar charmonium screening masses using periodic boundary conditions in the time direction. The comparison of the screening masses calculated with periodic and anti-periodic boundary conditions is shown in Fig. 3. As one can see from the figure there is no dependence on the boundary conditions in the low temperature phase of QCD. This is consistent with the fact that  $c\bar{c}$  pairs form bound states. For  $T_c < T < 1.5T_c$  we start seeing small differences in the screening masses calculated with periodic and anti-periodic boundary conditions. This might be an indication of broadening of the  $1S$  charmonium state. At temperatures  $T > 1.5T_c$  we already see a



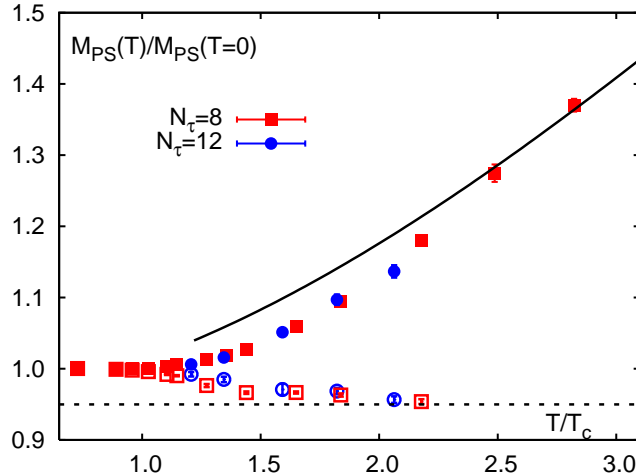


FIG. 3: Pseudo-scalar charmonium screening masses calculated with anti-periodic (filled symbols) and periodic (open symbols) boundary conditions as function of the temperature. Solid (dashed) lines correspond to the free theory prediction with  $m_c = 1.42$  GeV for anti-periodic (periodic) boundary conditions.

strong dependence on the boundary conditions indicating that the fermionic sub-structure of  $c\bar{c}$  pairs becomes relevant and the charm quark and anti-quark start becoming sensitive to the lowest Matsubara mode, which is non-zero in the case of anti-periodic boundary conditions. This is expected to happen when the bound state is dissolved. If periodic boundary conditions are used charmonium screening masses are equal to  $2m_c$  in the limit of very high temperature. If we choose  $m_c = 1.42$  GeV at the highest temperature we recover this expectation. Therefore, we used the value  $m_c = 1.42$  GeV when comparing with the free field theory prediction. Note, however, that for  $T > 2T_c$  the dependence of the screening masses on the boundary condition is compatible with the free theory expectation regardless what value of  $m_c$  is chosen; *i.e.* we can convert between the results obtained with periodic boundary condition to the ones obtained with anti-periodic boundary condition by simply adding the lowest Matsubara frequency in quadrature.

Let us comment on the behavior of the screening masses in other channels, *i.e.* for other choices of  $\tilde{\phi}(X)$ . The choice  $\tilde{\phi}(X) = -(-1)^{y+t}$  (or  $\tilde{\phi}(X) = -(-1)^{x+t}$ ) corresponds to  $\Gamma = \gamma_1$  (or  $\Gamma = \gamma_2$ ) in the non-oscillatory and  $\Gamma = \gamma_2\gamma_0$  (or  $\Gamma = \gamma_1\gamma_0$ ) in the oscillatory part, which in turn correspond to  $J/\psi$  and  $h_c$ , respectively. We have found that the correlator for this meson channel is dominated by the  $J/\psi$  and we were unable to obtain any signal

for the  $h_c$ . The qualitative behavior of the  $J/\psi$  screening masses was found to be quite similar to that of the  $\eta_c$  [29, 30]. Finally, for  $\Gamma = 1$  a pseudo-scalar ( $\eta_c$ ) and a scalar ( $\chi_{c0}$ ) states contribute to the non-oscillatory and oscillatory parts of the correlator. Similarly the choice  $\tilde{\phi}(X) = -(-1)^y$  (or  $\tilde{\phi}(X) = -(-1)^x$ ) corresponds to  $\gamma_2\gamma_3$  (or  $\gamma_1\gamma_3$ ) and  $\gamma_2\gamma_5$  (or  $\gamma_1\gamma_5$ ). Thus vector ( $J/\psi$ ) and axial-vector ( $\chi_{c1}$ ) states correspond to the non-oscillatory and oscillatory parts of the correlator. Contrary to the situation with light quarks, all three channels remain to receive both, non-oscillatory and oscillatory contributions above  $T_c$ . In fact, up to temperatures of about  $2T_c$  the non-oscillatory part is larger. Thus the screening masses corresponding to the non-oscillatory part of the correlators can be reliably calculated and show a temperature dependence that is very similar to that of the pseudo-scalar ( $\eta_c$ ) and vector ( $J/\psi$ ) screening masses discussed above. On the other hand, the scalar and axial-vector screening masses could be reliably determined only at temperatures  $T > 2T_c$ . At these temperatures they are consistent with the free theory value.

#### IV. CONCLUSIONS AND OUTLOOK

In this paper we have demonstrated that spatial charmonium correlators are useful tools for studying in-medium charmonium properties and their possible dissolution in the deconfined phase. The pseudo-scalar screening masses become temperature dependent just above the crossover temperature of  $2 + 1$  flavor QCD indicating that medium modifications of the charmonium spectral function set in gradually. At temperatures  $T > 1.5T_c$  we see already large modifications of the charmonium correlators, and the temperature dependence of the screening masses is qualitatively the same as the behavior expected for unbound  $c\bar{c}$  pairs. At  $T > 2T_c$  the value of the screening mass and its dependence on the boundary conditions is in agreement with the free field limit indicating the absence of charmonium states at these temperatures. The lattice results presented here are consistent with the expectation based on potential model and can be used to further constrain potential model calculations of the charmonium spectral functions. This, of course, will require that those calculations are extended to finite spatial momentum.

The investigations presented in this paper can be extended in different ways. While above the transition temperature cutoff effects are under control, this is not the case in the hadronic phase. To reduce the cutoff effects at low temperatures calculations using the

Highly Improved Staggered Quark (HISQ) [46] action will be necessary. The HISQ action can also reduce cutoff effects in the light quark sector. It would be furthermore interesting to do the calculations with a Wilson type action for heavy quarks, like the Fermilab action [47]. Since in this case scalar and axial-vector do not have to be disentangled from S-wave states this would presumably allow for a more accurate study of the P-wave charmonia.

### Acknowledgments

This work has been supported by the U.S. Department of Energy under Contract No. DE-AC02-98CH10886 and the European Union under grant agreement number 238353. The numerical computations have been carried out on the apeNEXT computer at Bielefeld University, QCDOC computers of the RIKEN-BNL research center and the USQCD collaboration at BNL and the BlueGene/L at the New York Center for Computational Sciences (NYCCS). We thank S. Datta for providing the code for the screening mass calculations for QCDOC as well as for the critical comments on the manuscript. We also thank G. Aarts for his very useful comments and discussions.

- 
- [1] T. Matsui and H. Satz, *Phys. Lett. B* **178**, 416 (1986).
  - [2] N. Brambilla *et al.* *Eur. Phys. J. C* **71**, 1534 (2011).
  - [3] A. Bazavov, P. Petreczky and A. Velytsky, *Quark Gluon Plasma 4*, p. 61, World Scientific 2010, Eds. R.C. Hwa, X.-N. Wang [arXiv:0904.1748 [hep-ph]];  
R. Rapp and H. van Hees, *ibid.* p. 111.
  - [4] R. Arnaldi *et al.* (NA60 Collaboration), *Nucl. Phys. A* **783**, 261 (2007).
  - [5] R. Granier de Cassagnac, *J. Phys. G.* **35**, 104023 (2008).
  - [6] P. Pillot (ALICE Coll.), arXiv:1108.3795 [hep-ex];  
G. Aad *et al.* (Atlas Coll.), *Phys. Lett. B* **697**, 294 (2011);  
C. Silvestre (CMS Coll.), arXiv:1108.5077 [hep-ex].
  - [7] M. Asakawa, T. Hatsuda and Y. Nakahara, *Prog. Part. Nucl. Phys.* **46**, 459 (2001).
  - [8] I. Wetzorke *et al.*, *Nucl. Phys. Proc. Suppl.* **106**, 510 (2002).
  - [9] T. Umeda *et al.*, *Eur. Phys. J. C* **39S1**, 9 (2005).

- [10] M. Asakawa and T. Hatsuda, Phys. Rev. Lett. **92**, 012001 (2004).
- [11] S. Datta *et al.*, Phys. Rev. D **69**, 094507 (2004).
- [12] A. Jakovac *et al.*, Phys. Rev. D **75**, 014506 (2007).
- [13] G. Aarts *et al.*, Phys. Rev. D **76**, 094513 (2007).
- [14] H. Iida *et al.*, Phys. Rev. D **74**, 074502 (2006).
- [15] H. Ohno *et al.* (WHOT-QCD Collaboration), arXiv:1104.3384 [hep-lat].
- [16] T. Umeda, Phys. Rev. D **75**, 094502 (2007).
- [17] P. Petreczky, Eur. Phys. J. C **62**, 85 (2009).
- [18] H. -T. Ding *et al.*, PoSLATTICE **2010**, 180 (2010).
- [19] G. Aarts, S. Kim, M. P. Lombardo, M. B. Oktay, S. M. Ryan, D. K. Sinclair and J. - I. Skullerud, Phys. Rev. Lett. **106**, 061602 (2011)
- [20] O. Kaczmarek *et al.*, Phys. Lett. B **543**, 41 (2002); Phys. Rev. D **70**, 074505 (2004) [Erratum-  
ibid. D **72**, 059903 (2005)]; P. Petreczky and K. Petrov, Phys. Rev. D **70**, 054503 (2004);  
O. Kaczmarek and F. Zantow, Phys. Rev. D **71**, 114510 (2005).
- [21] S. Digal *et al.*, Phys. Rev. D **64**, 094015 (2001).
- [22] A. Mocsy and P. Petreczky, Phys. Rev. Lett. **99**, 211602 (2007); Phys. Rev. D **77**, 014501  
(2008); Phys. Rev. D **73**, 074007 (2006).
- [23] D. Blaschke *et al.*, Eur. Phys. J. C **43**, 81 (2005).
- [24] M. Laine *et. al.*, JHEP **0703**, 054 (2007).
- [25] N. Brambilla *et al.*, Phys. Rev. D **78**, 014017 (2008).
- [26] C. Miao, A. Mocsy and P. Petreczky, Nucl. Phys. A **855**, 125 (2011);  
M. Margotta *et al.*, Phys. Rev. D **83**, 105019 (2011).
- [27] F. Riek and R. Rapp, New J. Phys. **13**, 045007 (2011).
- [28] G. Boyd *et al.*, Z. Phys. C **64**, 331 (1994).
- [29] S. Mukherjee, Nucl. Phys. A **820**, 283C (2009).
- [30] S. Mukherjee, PoSCONFINEMENT **2008**, 116 (2008).
- [31] M. Cheng *et al.*, Eur. Phys. J. C **71**, 1564 (2011).
- [32] U. M. Heller, F. Karsch and B. Sturm, Phys. Rev. D **60**, 114502 (1999).
- [33] F. Karsch, E. Laermann and A. Peikert, Nucl. Phys. B **605**, 579 (2001).
- [34] M. Cheng *et al.*, Phys. Rev. D **77**, 014511 (2008).
- [35] A. Bazavov *et al.*, Phys. Rev. D **80**, 014504 (2009).

- [36] A. Gray *et al.*, Phys. Rev. D **72**, 094507 (2005).
- [37] R. Sommer, Nucl. Phys. B **411**, 839 (1994).
- [38] M. Cheng *et al.*, Phys. Rev. D **74**, 054507 (2006).
- [39] A. Bazavov *et al.*, Phys. Rev. D **85**, 054503 (2012).
- [40] M. Cheng, PoSLATTICE **2007**, 173 (2007).
- [41] M. Cheng, Ph.D Thesis, “The QCD equation of state with charm quarks from lattice QCD,” (2008), AAT-3333321.
- [42] H. Kluberg-Stern *et al.*, Nucl. Phys. B **220**, 447 (1983).
- [43] M. F. L. Golterman, Nucl. Phys. B **273**, 663 (1986).
- [44] R. Altmeyer *et al.*, Nucl. Phys. B **389**, 445 (1993).
- [45] W. Florkowski and B. L. Friman, Z. Phys. A **347**, 271 (1994).
- [46] E. Follana *et al.* [HPQCD and UKQCD Collaborations], Phys. Rev. D **75**, 054502 (2007).
- [47] A. X. El-Khadra, A. S. Kronfeld and P. B. Mackenzie, Phys. Rev. D **55**, 3933 (1997).